Cavities for light and sound: a cavity-enhanced platform for quantum acoustics

Fisicaro, M.

1 Introduction

Surface acoustic waves (SAWs) are a particular type of mechanical waves that are confined to the surface of a material. These waves occur in nature during earthquakes, and they are responsible for most of the destruction associated with them. In contrast to these catastrophic events, well-controlled miniature versions of these *earthquakes* play an essential role in modern technologies such as telecommunication devices. If you own a smartphone, it's very likely that several miniature earthquakes are generated right now inside your pocket.

Unlike large-scale earthquakes, where surface acoustic waves typically have sub-Hertz frequencies, kilometer-sized wavelengths, and displacement amplitudes reaching meters, the surface acoustic waves generated in your smartphone have GHz frequencies, micrometer-sized wavelengths, and sub-nanometer displacement amplitudes. To put the difference in perspective, the disparity in the amplitudes of these two types of waves is comparable to the difference in size between a human and an atom. In this thesis, we will focus on the second kind, and in particular on Rayleigh waves, which is a type of surface wave whose existence was predicted by Lord Rayleigh in 1885 [1].

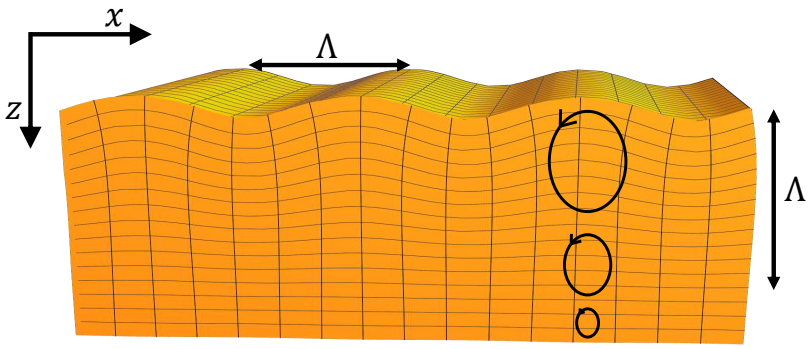

Figure 1.1: A Rayleigh wave of wavelength Λ decays with penetration into the material.

These waves are confined to the surface of the host medium, with a displacement amplitude that decays exponentially with the penetration into the material, vanishing at a distance of about one acoustic wavelength from the surface. In particular, the surface displacement has two components, one perpendicular to the surface, and one along the propagation direction of the waves, with a phase difference between the two that results in an elliptical motion of a volume element, as shown in Fig. 1.1.

Besides the surface confinement, which allows these waves to propagate over long distances, they have other characteristics that make them widely employed in modern technologies. They can be easily excited on piezoelectric materials by using interdigitated comb-shaped metal electrodes called interdigital transducers (IDTs), which are easy to fabricate with standard lithographic processes such as e-beam lithography. Due to the low speed of sound in solids compared to the speed of light, these waves have micrometer wavelengths at gigahertz frequencies, which makes them suitable for miniaturization

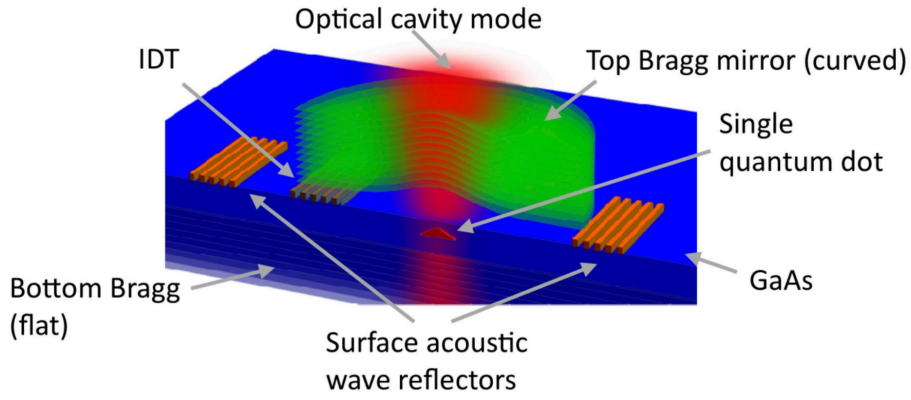

Figure 1.2: Conceptual illustration of a platform that allows confined SAWs on GaAs to interact with InGaAs quantum dots, which can be optically read out.

of electronic devices such as filters, delay lines, oscillators, and other signal-processing devices [2–8]. Due to their surface propagation, these waves can strongly interact with molecules, particles, and cells in contact with the free surface, enabling the sensing and manipulation of chemical substances and biological matter [6, 9–14].

Over the past two decades, SAWs have also started to be employed in quantum technologies and research due to their ability to interact with a variety of different quantum systems such as semiconductor quantum dots (QDs) [15–21], superconducting qubits [22–25], and defect centers [26–28]. Due to this range of interactions, SAWs have been proposed for a universal quantum transducer [29], and can be used in hybrid quantum systems [30, 31] to enable quantum transduction, for example, between microwave and optical photons [32–37]. The intrinsic surface confinement allows SAWs to propagate long distances with little dissipation, also enabling quantum protocols relying on propagating phonons [38–40].

This PhD project is intended to be the starting point to expand the research conducted at Leiden University into the field of quantum acoustics. For this purpose, this project primarily focuses on developing a platform where SAWs on GaAs interact with InGaAs quantum dots, which in turn can be optically read out. This can be achieved by confining the SAWs within an acoustic microcavity, and the quantum dots within an open-access optical microcavity, as shown in Fig. 1.2. In the rest of this introduction we will break down the individual components that constitute this platform.

1.0.1 Generation of surface acoustic waves

SAWs can be efficiently excited on a piezoelectric material using an interdigital transducer (IDT). Invented in 1965 by White and Voltmer [41], this transducer consists of two comb-shaped metal electrodes patterned on a piezoelectric material and allows the conversion of electrical energy into mechanical waves through the inverse piezoelectric effect. The same transducer can also detect surface waves via the direct piezoelectric effect, which converts mechanical energy back into an electrical signal.

The simplest IDT geometry is illustrated in Fig. 1.3, where two adjacent fingers belonging to the different metal combs form the unit cell of the IDT. This unit cell is characterized by the width of the electrodes d which, in this case, is equal to half the pitch p (center-to-center distance between two adjacent fingers), the length L of the fingers, and the acoustic aperture W, which corresponds to the overlap between the fingers

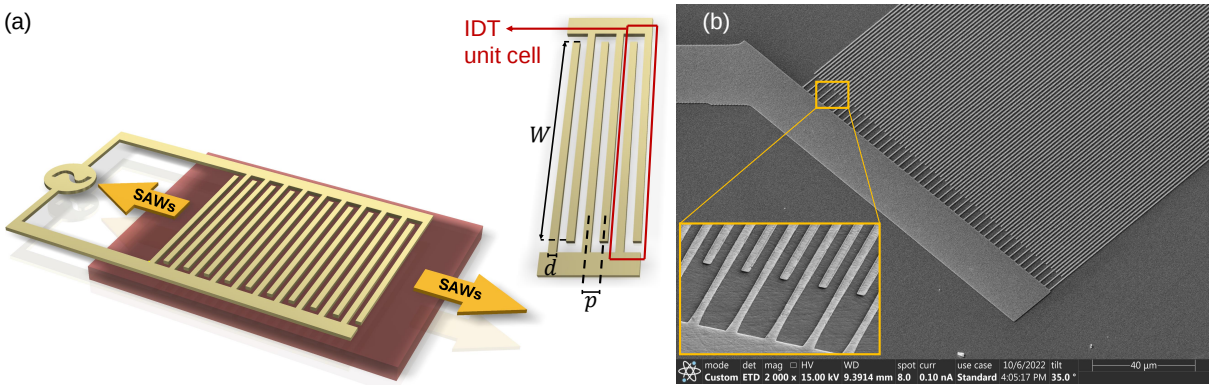

Figure 1.3: Interdigital transducer (IDT). (a) Sketch of a bidirectional interdigital transducer. (b) Scanning electron microscope picture of an IDT fabricated on GaAs by metal deposition of aluminium, with $d = 700\,\text{nm}$, $p = 1.4\,\mu\text{m}$ for a design wavelength $\Lambda = 2.8\,\mu\text{m}$.

in the transverse direction of the IDT.

The repetition of this unit cell forms the complete IDT, where N_f is the total number of finger pairs. The fingers on the same comb are connected via metal bus bars, to the signal and ground electrodes. The pitch p, together with the phase velocity of SAWs v_{SAW}, defines the central (or synchronous) frequency of the IDT $f_0 = v_{SAW}/2p$. Applying a voltage signal at this frequency results in constructive interference between the waves generated by individual unit cells of the IDT, thereby generating stronger SAWs. The amplitude of the generated SAWs is approximately proportional to the number of finger pairs in the IDT N_f. While increasing the number of finger pairs might seem advantageous, it also affects the frequency bandwidth of the IDT. The 3 dB frequency bandwidth is $\Delta f \simeq f_0 \times 0.885/N_f$ [42].

The IDTs described in this thesis, are aluminium IDTs with $N_f = 10$, fabricated on (001)-cut GaAs, and oriented along the [110] direction, for which the phase velocity of SAWs is $v_{SAW} = 2865\,\text{m/s}$ [43]. The pitch is $p = 1.4\,\mu\text{m}$, resulting in a synchronous frequency $f_0 \simeq 1.02\,\text{GHz}$ and a 3 dB frequency bandwidth of $\Delta f \simeq 90\,\text{MHz}$. The width of the fingers is $d = 700\,\text{nm}$, the finger length $L = 313\,\mu\text{m}$, and the acoustic aperture $W = 304\,\mu\text{m}$, resulting in low beam diffraction [8]. The thickness of the aluminium is kept below 100 nm for the devices presented in this work.

The IDT described above is the simplest realization of a SAW transducer, and corresponds to a bidirectional transducer, since it equally excites surface acoustic waves traveling in both directions. In this thesis, we use this configuration, although other geometries, such as unidirectional transducers [44, 45], or focusing IDTs [46, 47], are also possible.

1.0.2 Acoustic cavities and phonon confinement

Acoustic mirrors can be arranged to form an acoustic Fabry-Perot cavity, providing additional in-plane confinement to the SAWs. These mirrors are realized by periodically modulating the mechanical impedance of the surface on which the waves travel akin to a *distributed Bragg reflector* (DBR), either with grooves etched in the piezoelectric material or with metal gratings equivalent to short-circuited IDTs [29]. In our case, we use metal gratings with fingers having the same parameters as the IDTs. In this configuration, the

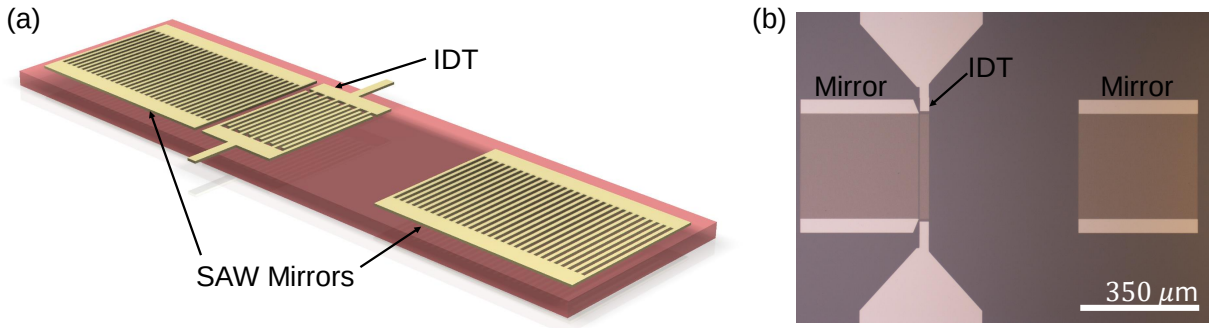

Figure 1.4: (a) Illustration of a SAW acoustic cavity with embedded IDT (1-port resonator). (b) Optical microscope image of a SAW cavity on GaAs.

center frequency of the SAW mirror is given by $f_0 = v_{SAW}/2p$, where p is the grating pitch and v_{SAW} is the phase velocity of SAWs in the mirror. The excitation of SAWs is provided by an IDT, typically embedded in the cavity. The same IDT can be also used for detecting SAWs, and in this case, the device is called a 1-port resonator, as illustrated in Fig. 1.4.

The total reflectivity of the mirror depends both on the reflectivity of a single finger r_s and on the total number of fingers in the mirror N_m. While the geometrical cavity length L_c is given by the separation between the two mirrors, the effective cavity length is larger, due to the exponential decay of the acoustic field in the mirrors $L_{eff} = L_c + 2L_p$, where L_p is the penetration depth inside the mirrors. The cavity can then be modeled as two thin reflectors separated by a distance L_{eff}.

The interaction between a single phonon and other quantum systems depends on the displacement associated with the single phonon. This is given by the zero-point mechanical motion $U_0 = \sqrt{\hbar/(2m_{eff}f_0)}$, where $\hbar$ is the reduced Planck constant, m_{eff} is the effective mass of the mechanical mode, and f_0 is its frequency. An approximation of m_{eff} for surface acoustic waves can be given in terms of material density ρ and mode volume V. Assuming that the penetration depth of SAWs into the material is approximately one acoustic wavelength Λ we obtain

$$U_0 \simeq \sqrt{\frac{\hbar}{2\rho v_{SAW} A}}\,, \tag{1.1}$$

where A is the surface area on which the phonon is confined. Taking into account the mode shape and material properties, the estimate for GaAs is $U_0 = 1.9\,\mathrm{fm}/\sqrt{A[\mu\mathrm{m}^2]}$ [29], where A is the area of the cavity, expressed in $\mu\mathrm{m}^2$.

From this, it is clear that to achieve high coupling of phonons with other quantum systems, a SAW cavity should not only have high quality factor Q, but also a low mode volume. In principle, we can reduce the mode volume by employing gratings with higher metal thickness h, which increases the single finger reflectivity r_s and, with this, reduces the penetration depth of the acoustic field inside the mirrors.

For a highly reflective mirror, the penetration depth is indeed related to the single finger reflectivity by $L_p \simeq \Lambda/(4|r_s|)$ [29,48], where Λ is the acoustic wavelength and $|r_s| = C_1(h/\Lambda)\sin(\pi d/p) + C_2(h/\Lambda)^2\cos(\pi d/p)$, with $C_{1,2}$ being material-dependent prefactors [49]. However, increasing the metal thickness also increases losses in the mirrors via scattering of surface waves into bulk waves (bulk losses) proportional to $(h/\Lambda)^2$ [50], so

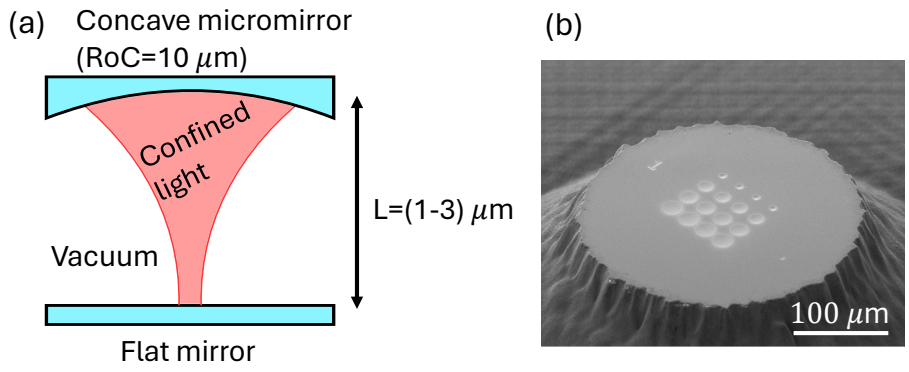

Figure 1.5: (a) Sketch of the open-access optical microcavity, with plano-concave mirrors configuration. (b) Scanning electron microscope image of the micromirror array used for our cavity. The concave mirrors have radii of curvature (RoC) ranging from 100 to 10 μm.

a compromise must be found to achieve high-quality factors while maintaining low mode volume.

Finally, we note that there are other contributions to losses in the acoustic cavity, such as radiation through the mirrors, diffraction, and material losses [29,49]. The contribution of the bulk losses is negligible at room temperature, due to much higher material losses, but it becomes problematic at cryogenic temperatures where material losses have been minimized.

Planar cavities at GHz frequencies with quality factors of $Q \sim 10^5$ have been achieved on GaAs at mK temperatures, but only with a cavity length of several hundred micrometers [51]. For shorter effective cavity lengths of $L_{eff} \sim 40\Lambda$, quality factors of $Q \sim 10^3$ are achievable [29]. To achieve an even smaller cavity surface area A, different cavity geometries are needed to provide confinement also in the transverse direction. With concave cavities, for example, it is possible to achieve $A \simeq (40 - 200)\,\mu\text{m}^2$, corresponding to single phonon displacements $U_0 \simeq (0.1 - 0.3)\,\text{fm}$ [15, 20, 29, 52].

1.0.3 QD interaction: optical microcavities

As seen in the previous section, the coupling between SAW phonons and other quantum systems depends on the displacement associated with a single phonon. In a piezoelectric material, SAWs have an associated strain and electric field that allow them to interact with semiconductor quantum dots, if they are located close to the surface. In future experiments, we aim to couple SAWs with InGaAs quantum dots (QDs) in a GaAs substrate, which is possible via the modulation of the energy levels of the QDs induced both by the deformation potential (SAW strain) and by the quantum-confined Stark effect (SAW electric field) [19].

To enable applications such as single phonon detection and microwave-to-optical quantum transduction, it is desirable to place the interacting QD-SAW system in an optical microcavity, to boost the optical readout and enhance the spontaneous emission of the QD into the optical cavity modes [53–56].

Due to the free-surface requirement needed to generate SAWs, a suitable type of optical microcavity are open-access microcavities, a miniaturized version of Fabry-Perot optical cavities. Here two mirrors, where at least one has a micrometer-scale curvature, are

separated by an air or vacuum gap and can be positioned with very high precision at a micrometer distance, to form a cavity as shown in Fig. 1.5.

Despite the high tunability provided by these cavities, which allows to be used them in high-efficiency single-photon sources [56, 57], these cavities do not have a high mechanical stability, as the two mirrors are not integrated in the same monolithic structure and can move with respect to each other in the presence of external mechanical vibrations. While this is not a significant problem in helium bath cryostats, which can be made mechanically quiet, resulting in very high mechanical stability of the cavity with root mean square (rms) fluctuation of the cavity length down to 4.3 pm [58], it hinders the operation in closed-cycle cryostats.

To circumvent this problem, low-pass mechanical filters have been employed in these cryostats, to allow the operation of fiber-based open-access microcavities with cavity length fluctuations of 15 pm rms in non-contact mode, down to 0.8 pm rms when the two mirrors are in direct contact [59]. However, this design is not easily compatible with free-space optical coupling to the cavity, since the presence of a mechanical low-pass filter in the cryostat gives rise to time-dependent fluctuations of the optical power coupled to the cavity.

In chapter 5, we focus on the development of a highly stable open-access microcavity for operation in a standard closed-cycle cryostat with free-space optical coupling. In particular, we demonstrate the operation of an open-access microcavity with high mechanical stability, by using standard active feedback stabilization, without the use of a dedicated mechanical low-pass filter [60]. This is an important step towards the commercialization of quantum technologies since closed-cycle cryostats are turnkey systems that require minimal maintenance and have high portability.

1.0.4 Thesis outline

The project presented in this thesis aims to develop a platform for quantum acoustics experiments where surface acoustic wave (SAW) phonons interact with InGaAs quantum dots (QDs). To enhance the phonon-QD interaction, GHz acoustic cavities were nanofabricated on a GaAs substrate, which will also host the quantum dots in future experiments. Additionally, to enhance the photon-QD interaction, and to improve the optical readout of the quantum dot, an open-access optical microcavity with high mechanical stability was constructed within a closed-cycle cryostat.

While the nanofabrication of the planar SAW cavities is in principle a straightforward process, their characterization is found to be more intricate. The conventional approach involves using the interdigital transducer (IDT) for both excitation and detection of the SAWs, measuring the microwave reflectance spectrum with a vector network analyzer (VNA), and providing information on the position of the resonance frequencies. However, due to the transverse extension of the IDT across the entire cavity, this method does not offer insights into the acoustic field distribution within the cavity. Although adequate for ideal systems with frequency and spatially separated resonances, this approach complicates the interpretation of results in real cavities. For this reason, our focus shifted towards the development of an imaging system capable of measuring the spatial distribution of GHz surface acoustic waves both in amplitude and phase.

In **Chapter 2** we introduce this system: a fiber-based scanning Michelson interferometer for imaging GHz surface acoustic waves. Specifically, we demonstrate the accurate measurement of out-of-plane surface displacement using a focused laser beam with a beam

spot size matching the surface acoustic wavelength. With this setup, we investigate a 1-port GHz SAW resonator on GaAs and compare the results with VNA measurements. We show that by imaging the amplitude and phase of the surface displacement, we can distinguish between frequency and spatially overlapping transverse modes. Understanding the distribution of the acoustic field inside the cavity is crucial for future interaction with localized quantum dots.

In **Chapter 3** we employ the scanning Michelson interferometer to analyze interference fringes in GHz surface acoustic wave cavities. In particular, we investigate the presence of spurious bulk acoustic waves (BAWs) in SAW cavities, using two-dimensional spatial Fourier analysis. While BAWs can be readily detected by imaging the amplitude and phase of the acoustic field distribution, we demonstrate that this is also achievable with amplitude-only measurements, due to the interference between bulk and surface waves. This method can be valuable for optimizing SAW cavities, as the scattering of surface waves into bulk waves constitutes a loss mechanism.

In **Chapter 4** we demonstrate the optical Talbot effect by diffraction of light from standing surface acoustic waves, which behave as a dynamical diffraction grating.

In **Chapter 5** we present the realization of an open-access optical microcavity with high mechanical stability in a standard closed-cycle cryostat. Our setup features free-space optical coupling and is carefully designed to allow cavity-length stabilization using conventional feedback techniques, removing the need for a dedicated mechanical low–pass filter in the cryostat.